

Chapter 1

Introduction

For many decades, miniaturization has been one of the main driving forces in scientific and economic progress. In the year 2003, lithographical miniaturization, as measured by the *DRAM half pitch*¹ has reached the 100 nm mark and is supposed to continue shrinking².

But with the decreasing feature size new problems are arising. The stability of the smaller structures is decreasing. Going hand in hand with this, the amount of defective structures rises. Another main problem of nowadays electronical devices, emerging from the increased power density, is their high power consumption and heat dissipation.

Therefore, there is a vast interest in finding new approaches to miniaturization that can overcome the aforementioned problems. One of these approaches takes advantage of an effect well-known from biology: the self-assembling capability of organic molecules. While nowadays devices and circuits are built by the so-called “top-down” approach (which means that structures are created out of bigger building blocks, e.g. by lithographic structuring), organic molecules can assemble on technological relevant surfaces, e.g. metal surfaces, without further need of manual construction into highly complex structures, driven only by intermolecular binding forces (“bottom-up” approach). Here, each molecule serves as a unique building block that can be functionalized by chemical synthesis, which makes it possible to control the properties of the eventually assembled structures. Because organic molecules are about a factor of 20 smaller than the smallest structures fabricated nowadays by the “top-down” approach, and because they can be pro-

¹The *DRAM half pitch* is the average of half the distance between two metal lines connecting the cells of a DRAM memory device. The factor 1/2 takes care of the fact, that the distance also includes the free space between the lines.

² http://www.itrs.net/Links/2004Update/2004_01_Design.pdf,
http://www.itrs.net/Links/2006Update/FinalToPost/02_Design_2006Update.pdf

duced in vast amounts with only a small number of defects and sometimes even self-healing capabilities, the “bottom-up” approach is widely believed to be the next step in the miniaturization process.

However, there is still a lot of knowledge to be gathered in order to fully control the self-assembling process. Although in solution and the bulk state chemists have developed highly sophisticated methods, it turns out that it is difficult to transfer these principles to surfaces, where the motional degree of freedom is limited to two dimensions and interactions with the substrate influence the system. Therefore, a good understanding of the self-assembly process on surfaces is a key for building technologically relevant, functional devices via the “bottom-up“ approach.

In this thesis, different principles to control the self-assembly behavior of porphyrin derivatives are studied. The results are presented in section 3, after in section 2 a brief introduction into the applied methods and materials is presented. In section 3.1 it will be shown that with the same molecular building block either one-dimensional wires or two-dimensional nanoporous networks can be formed on the same substrate depending on the molecular coverage. By subtle changes of the molecular architecture, furthermore the pore-to-pore distance inside these networks will be altered. In section 3.2 such a nanoporous network will be used as the basis for a fully self-assembled supramolecular device. The characteristics of the device, especially its behavior at different temperatures and the activation energy for rotation, will be studied in detail. It will be shown that an individual device can be addressed and operated by the tip of a Scanning Tunneling Microscope (STM). Finally, in section 3.3 bimolecular systems are investigated. Here it will be shown how the balance between entropy and enthalpy can be used to form intermixed networks. These types of network are widely believed to be a key to the understanding of the self-assembly process.

Chapter 2

Methods and Materials

2.1 Scanning Tunneling Microscopy

Invented in 1981 by Gerd Binnig and Heinrich Rohrer at the IBM Zürich Research Laboratory,^[1, 2] the Scanning Tunneling Microscope (STM, which is also the abbreviation for scanning tunneling microscopy) has become a powerful tool for studies at the nanoscale. STM is a real-space method, which circumvents the rather complicated interpretations of experiments in the reciprocal space. Because of its high resolution, even single atoms can be made visible³. Furthermore, STM experiments yield information about the local characteristics of the probed sample and do not provide mean values over rather large areas. Next to its imaging power, the STM bears spectroscopical capabilities and even allows for the manipulation of single atoms or molecules. Therefore, the STM has been the technique of choice for this thesis. However, as the STM is based on the quantum mechanical tunneling effect, it needs a conductive or semi-conductive surface as a substrate for the investigated samples.

2.1.1 Basic Theory

The STM consists mainly of a sharp metallic tip (preferentially with a mono-atomic apex) which is brought into close proximity (typically a few Å) of a (semi-) conductive surface. Based on the quantum mechanical tunneling effect, electrons can tunnel through the gap between tip and sample. By applying a small bias voltage (usually in the range of 0.01 to 3 V) a directed tunneling current occurs, which is highly depending on the distance

³Although there are hints that the resolution of the Atomic Force Microscope is even better and subatomic resolution can be achieved with it.^[3]

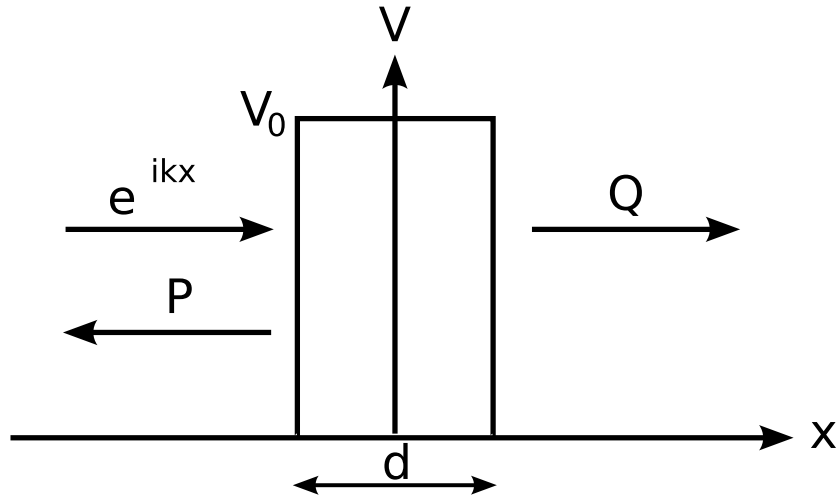


Figure 2.1: One-dimensional model for the quantum mechanical tunneling effect. A (particle) wave (e^{ikx} , coming from the left) faces a potential V_0 that is larger than the energy of the wave. In the classical case the wave is completely reflected by the potential: The propabilities to find the wave on either side of the potential are $P = 1, Q = 0$. Quantum mechanically the propability Q to detect the wave on the right side of the potential can be > 0 .

between tip and sample. Therefore, while the tip scans over the sample surface by means of piezo-electric actuators (x- and y-piezos) to obtain a two-dimensional map, even small corrugations lead to changes in the measured tunneling current. By another piezo-electric element (the z-piezo) the height of the tip above the sample can be varied.

Several different scanning modes are possible. In the *constant height* mode, the tip scans over the sample with the z-piezo held at a constant value while the current is being measured as reference signal. Alternatively, in the *constant current* mode a feedback system is used to keep the tunneling current constant. This is achieved by adjusting the tip-sample distance via the z-piezo. The changes in the z-direction are then taken as the reference signal. The latter mode also provides the possibility to scan over surfaces that are not perfectly horizontally aligned, but has the disadvantage of lower scanning speed. The *constant current* mode was used for all images taken in this thesis. To visualize the STM image, the recorded reference signal is depicted at every point of the two dimensional map by a pre-defined color code. In this thesis, the color code for each image was chosen in a way that darker colors reflect less height on the sample. However it has to be noted

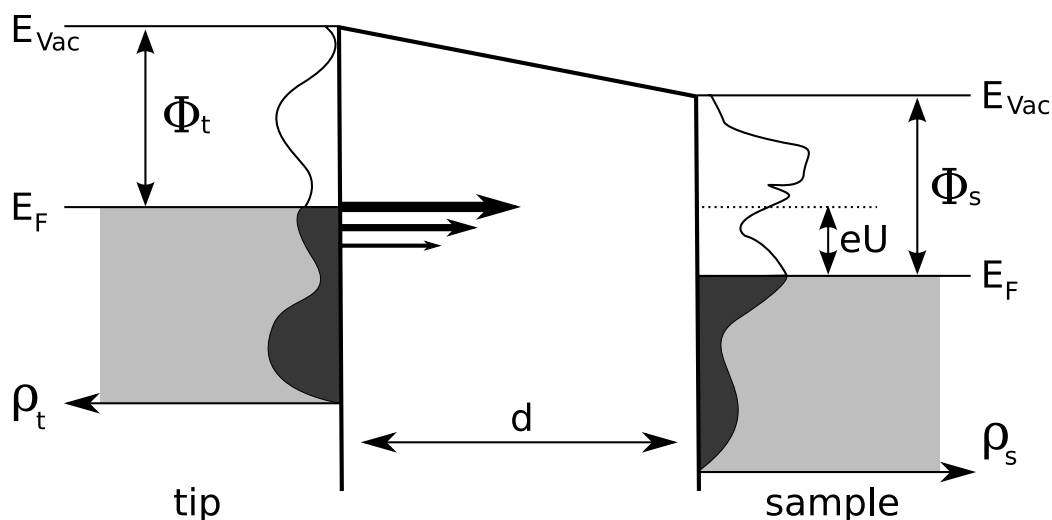


Figure 2.2: One-dimensional schematic energy diagram for tunneling from tip (grounded) to sample (positive bias voltage U applied). $\rho_{t,s}$ indicate the density of states and $\Phi_{t,s}$ the work function for the tip and the sample, respectively. The sizes of the arrows in the gap indicate that the probability for tunneling has its maximum at $E = eU$.

that in both scanning modes these maps are derived from the tunneling current and therefore resemble electronic rather than topographical features (see next section).

Mathematical Description of the Tunneling Process

Developing a precise mathematical description of the tunneling process in STM is tempting. The main problems are the unknown geometry of the tip (which may even change during one experiment) and its chemical composition. Nevertheless, applying some simplifications and assumptions, the basic aspects of the process can be explained.

When a macroscopic particle of mass m faces a potential V_0 that is greater than its energy E , the particle is reflected. But when the particle decreases to a size, where its wave character becomes recognizable, this classical description fails. In this region, the particle can, if the barrier width d is small enough, with a small probability Q tunnel through the energetically

forbidden region and be detected on the other side (Figure 2.1).⁴

$$Q = \exp\left(-\frac{2d}{\hbar}\sqrt{2m(V_0 - E)}\right) \quad (2.1)$$

In 1961 J. Bardeen discussed the tunneling process through the vacuum between two metal plates (Figure 2.2).^[5] Instead of solving the Schrödinger equation for the whole system, he divided it into two independent subsystems. In this one-dimensional theory the specific geometry of the gap is ignored. Fermi's golden rule, which describes the transition rate between two quantum states, gives the probability of an electron to elastically tunnel between a sample state at the surface and a tip state. The tunneling current I is directly proportional to the number of sample states at the surface within the energy interval eU .^[6] Using Bardeen's approach, it can be approximated as^[7, 8] (with the Fermi energy $E_F = 0$)

$$I \propto \int_0^{eU} dE \rho_t(E - eU) \rho_s(E) T(E, eU, d), \quad (2.2)$$

where U is the applied small bias voltage (with respect to the tip), and $\rho_{t,s}$ are the densities of states for the tip and the sample, respectively. $T(E, eU, d)$ is the transmission coefficient,

$$T(E, eU, d) = \exp\left(-\frac{2d}{\hbar}\sqrt{2m\left(\frac{\phi_t + \phi_s}{2} - \frac{eU}{2} - E\right)}\right), \quad (2.3)$$

where $\phi_{t,s}$ are the work functions for the tip and the sample, respectively.

According to equation 2.2, the tunneling current is simply an integral of the transmission coefficient multiplied with the densities of states $\rho_{t,s}$ (DOS) of the tip and the sample. However, this equation does not include the tip geometry. Therefore, the DOS of tip and sample are exchangeable. To apply Bardeen's theory to the STM, in 1983 J. Tersoff and N. D. Hamann approximated the tip apex as a metal sphere with only the s-states of the tip applying to the tunneling process.^[9, 10] According to their formula, the contribution of the tip to the tunneling current is only a constant value. Therefore, by detecting the tunneling current (equation 2.2), basically the local density of states (LDOS) of the sample is recorded. For metal surfaces, the LDOS reflects the surface topography in good agreement⁵, but for adorbates there may be vast differences (see section 2.1.2).

⁴A description of the tunneling effect can be found in many textbooks, for example in Ref.^[4]

⁵Although even for clean metal surfaces features like surface states lead to a difference between the topography and the LDOS.

The simple model of the Tersoff-Hamann theory failed in explaining the observed atomic resolution on close-packed metal surfaces.^[11] This was achieved in 1990 by C. J. Chen, who assumed a d_{z^2} -tip state.^[12, 13] A more detailed description of the tunneling process can be found in many books^[6, 11] and in a review by D. Drakova.^[14]

2.1.2 Imaging Molecules

The question whether it is possible to image organic adsorbates and molecules with the STM was relatively easily answered by the first successfully taken STM images in the mid 1980s.^[15, 16] Until then, doubts were being uttered related to the relatively large energy gap observed between the highest occupied molecular orbital (HOMO) and the lowest unoccupied molecular orbital (LUMO) compared to the low bias voltages applied in STM. This energy gap was thought to prevent the molecules from being imaged. But since the molecular orbitals (MO) interact with the metal surface's energy band, these MOs are altered^[17] such that imaging becomes possible. However, it also means that the HOMOs and LUMOs of adsorbed molecules can differ from those of isolated ones.

Many effects can influence the appearance of adsorbates in STM images⁶. Depending on the applied bias voltage, different MOs can contribute to the tunneling current. For example, on a titanium film O_2 looks like a protrusion or, counterintuitively, like a depression.^[19] The adsorption site of the adsorbate on the surface has an influence on the adsorption state. For example, CO on Pt(111) appears either as a "bump" on on-top sites or as a sombrero-like shape on bridge sites.^[20] Also for larger adsorbates as organic molecules the appearance in STM images can depend on the applied voltage,^[21] the adsorption site,^[22] but also on the surface geometry.^[23] Furthermore, due to intermolecular interactions, a single molecule can look different from one embedded in a network (compare figures 3.1 and 3.2 in section 3.1.1). If the molecule diffuses or rotates much faster than the characteristic scanning speed of the STM (about a millisecond per pixel, depending on the scanning mode), it might be impossible to identify the molecule or its inner structure.^[24] Also, some side-groups, like alkyl-chains attached to a porphyrin ring, can continuously change their conformation while the molecular core itself is immobile on the surface. This can lead to (partly) fuzzy appearances in STM images, when the movement of such moieties is faster than the characteristic scanning speed of the STM. Furthermore, static conformational changes of the molecule's residues can lead to different appearances of

⁶A very good discussion of these effects can be found in a review by P. Sautet.^[18]